

Triplet spin resonance of the Haldane magnet $\text{PbNi}_2\text{V}_2\text{O}_8$ with interchain coupling

A. I. Smirnov,¹ V. N. Glazkov,¹ T. Kashiwagi,² S. Kimura,² M. Hagiwara,² K. Kindo,³ A. Ya. Shapiro,⁴ and L. N. Demianets⁴

¹*P. L. Kapitza Institute for Physical Problems, RAS, 119334 Moscow, Russia*

²*Center for Quantum Science and Technology under Extreme Conditions (KYOKUGEN), Osaka University, 1-3 Machikaneyama, Toyonaka, Osaka 560-8531, Japan*

³*Institute for Solid State Physics (ISSP), University of Tokyo, 5-1-5 Kashiwanoha, Kashiwa, Chiba 277-8581, Japan*

⁴*A.V. Shubnikov Institute for Crystallography, RAS, 117333 Moscow, Russia*

(Received 31 October 2007; revised manuscript received 21 January 2008; published 6 March 2008)

Spin resonance of the triplet excitations is studied experimentally in the Haldane magnet $\text{PbNi}_2\text{V}_2\text{O}_8$. The absorption spectrum has features of spin $S=1$ resonance in a crystal field, with all three components, corresponding to transitions $|\pm 1\rangle \rightleftharpoons |0\rangle$ and $|-1\rangle \rightleftharpoons |1\rangle$, being observable. The resonance field is temperature dependent, indicating the renormalization of excitation spectrum in the interaction between the triplets. Magnetic resonance frequencies and critical fields of the magnetization are consistent with a boson version of the macroscopic field theory [J. Affleck, Phys. Rev. B **46**, 9002 (1992); A. M. Farutin and V. I. Marchenko, Zh. Eksp. Teor. Fiz. **131**, 860 (2007)] [JETP **104**, 751 (2007)] while they contradict the fermion version and the previously used approach of noninteracting spin chains.

DOI: 10.1103/PhysRevB.77.100401

PACS number(s): 75.10.Jm, 75.40.Gb, 76.30.-v, 76.50.+g

The inorganic dielectric $\text{PbNi}_2\text{V}_2\text{O}_8$, with the magnetic structure formed by chains of Ni^{2+} ($S=1$) ions, exhibits a Haldane-like ground state.^{1,2} This quantum collective spin state is characterized by the absence of ordered spin components and by the energy gap, which separates magnetic excitations from the singlet ground state. Because of the energy gap, this kind of spin-liquid state is stable in the presence of weak anisotropy and interchain exchange. This differentiates chains of $S=1$ ions from $S=1/2$ spin chains, which are known to order due to interchain exchange. In $\text{PbNi}_2\text{V}_2\text{O}_8$, the anisotropy and interchain exchange reduce the Haldane gap, and the system is close to the critical point of the quantum phase transition from a spin-liquid to an ordered easy-axis antiferromagnet.³ Besides, the spin-liquid phase may become unstable at the critical magnetic field, corresponding to the vanishing of the energy gap of triplet excitations. In the exchange approximation, the critical field value H_c and the energy gap Δ are related by a simple relation $g\mu_B\mu_0H_c=\Delta$. The influence of the single-ion anisotropy on the Haldane state was analyzed theoretically by the exact diagonalization for finite chains,⁴ by a perturbative approach,^{4,5} and by macroscopic field-theory methods.⁶ In the magnetic field range far below H_c , all models result in the same energy levels, parametrized by the main gap, one or two anisotropy constants, and g factor. The perturbative description of excitations in the Haldane chain appears to be identical to that of an isolated spin $S=1$ in a crystal field.⁷ Extrapolated to the field of spin-gap closing, for the uniaxial case, the perturbative approach yields critical fields at the orientation parallel or perpendicular to the crystal axis:

$$g\mu_B\mu_0H_{c\parallel}=\Delta_{\perp}, \quad g\mu_B\mu_0H_{c\perp}=\sqrt{\Delta_{\parallel}\Delta_{\perp}}, \quad (1)$$

where Δ_{\perp} is the gap of $S_z=\pm 1$ triplet components with the momentum of π , and Δ_{\parallel} is the gap of $S_z=0$ triplet component.

The effect of magnetic field on the spectrum of the Haldane system was studied experimentally for

$\text{Ni}(\text{C}_2\text{H}_8\text{N}_2)_2\text{NO}_2(\text{ClO}_4)$. The spin gap, however, remained nonzero in that case due to the staggered g tensor.⁸ $\text{PbNi}_2\text{V}_2\text{O}_8$ is a convenient model system to study the influence of three-dimensional (3D) correlations and anisotropy on the spin gap in a magnetic field, because this compound demonstrates an anisotropic critical field, a spin-liquid behavior below the critical field, and a field-induced 3D antiferromagnetic ordering above H_c .⁹

The perturbative approach of noninteracting Haldane chains [formula (1)] was used¹⁰ for $\text{PbNi}_2\text{V}_2\text{O}_8$ to derive the energy gaps from the critical field values. Further, intrachain and interchain exchange integrals were found by fitting the inelastic neutron scattering intensity at fixed spin-gap values.^{1,2,10} Nevertheless, the extrapolation of the perturbative approach to high fields may be doubtful. While it is justified by the exact diagonalization of the finite chain problem,⁴ the bosonic version of the macroscopic field-theory treatment⁶ shows different results near the critical field. This model implies an interchain coupling of nearly a critical value, causing the 3D order. Another macroscopic theory, considering a general case of a spin-gap magnet with the field-induced 3D ordering, was developed in Ref. 11. The source Lagrangian and the critical fields in the bosonic model of Ref. 6 and in the macroscopic theory¹¹ are identical. The results of the fermionic model of Ref. 6 are close to the perturbative theory. Probably, the divergency of the results of the bosonic model from the perturbative curves near the critical field should be ascribed to fluctuations, which are suggested to be suppressed (e.g., by 3D coupling) in the boson model of Ref. 6 and in Ref. 11. The study of magnetic resonance spectra along with the magnetization curves should allow one to check the validity of the above models. In this Rapid Communication, we study the triplet excitations by means of the high-frequency electron spin resonance (ESR) spectroscopy, which enables one to measure directly the frequencies of the transitions between triplet sublevels. We recover the splitting of the zero-field energy gap from ESR experiment and relate it to the difference between the

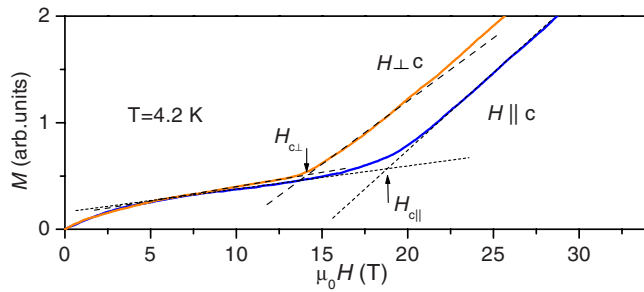


FIG. 1. (Color online) Pulse field magnetization of the aligned sample of $\text{PbNi}_2\text{V}_2\text{O}_8$. Solid curves, experiment; dashed straight lines, extrapolations to determine $H_{c\perp, \parallel}$.

critical fields $H_{c\perp}$ and $H_{c\parallel}$. The observed splitting of triplet sublevels strongly contradicts the perturbative relation (1). At the same time, the spectrum of triplet excitations is well described by macroscopic models, implying 3D ordering at the critical field.^{6,11} Thus, the interchain coupling should be important for the magnetic excitations.

We used ceramic samples of $\text{PbNi}_2\text{V}_2\text{O}_8$ prepared as described in Ref. 12 and samples aligned by a magnetic field, prepared following Ref. 1, with the orientation of the tetragonal axis (c axis) of crystallites parallel to the aligning field. Magnetization curves taken by the pulse technique are shown in Fig. 1. The critical field values derived from these curves are $\mu_0 H_{c\parallel} = 19 \pm 0.5$ T and $\mu_0 H_{c\perp} = 14 \pm 0.5$ T, which are well consistent with the data of Refs. 1 and 9. The ESR spectra were measured both for ceramic and aligned samples as microwave transmission vs magnetic field dependences. Magnetic field was created by a 16 T cryomagnet. Microwave signal in the range 70–500 GHz was generated and detected by means of the vector network analyzer from the ABmm system at the KYOKUGEN Center.

A typical ESR signal of an aligned sample and its evolution with temperature are presented in the main panel of Fig. 2. At the temperature above 35 K, there is a single ESR line, corresponding to an exchange-narrowed Ni^{2+} ESR signal with g -factor value of 2.23. On cooling the sample, the absorption at this resonance field diminishes and, in addition, there appear three ESR lines (marked as A, B, and C) apart from the high-temperature position. At low temperatures, the lines A–C disappear again and a residual absorption in the range 8.6–10.5 T ($g=1.9$ –2.2) is observed, with the maximum at 8.8 T ($g=2.2$). The intensity of this low-temperature signal grows with defect concentration¹² and, thus, can be attributed to defects and impurities. It grows on cooling, like the ESR of paramagnetic impurities, and corresponds to the increase of the magnetic susceptibility at low temperatures (not shown here). On the contrary, as mentioned above, lines A–C vanish below 7 K. The drop of the intensity of lines A and B may be followed in the main panel of Fig. 2, while line C at this frequency is superimposed with ESR of defects at 10.5 T. However, it can be resolved by changing frequency, as shown in the lower inset of Fig. 2. Then it is clear that this component also disappears on cooling below 4 K. The resonance fields H_A , H_B , and H_C of the lines A, B, and C are temperature dependent, as shown in the upper inset of Fig. 2. The increase of signals A–C with heating between 7

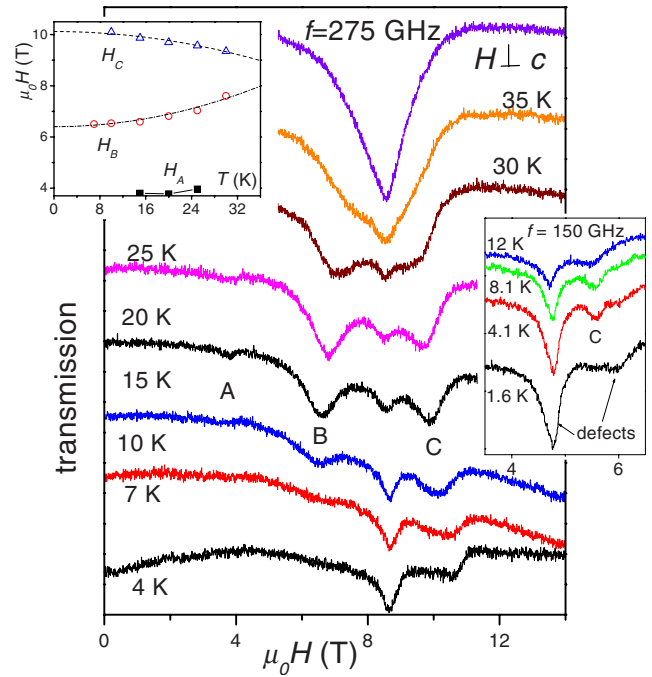


FIG. 2. (Color online) 275 GHz ESR spectra of a $\text{PbNi}_2\text{V}_2\text{O}_8$ aligned sample measured at different temperatures for H perpendicular to the alignment axis. Upper inset: Temperature dependence of the ESR fields A, B, and C. $f=275$ GHz. Lines are a guide for the eye. Lower inset: 150 GHz ESR of a ceramic sample.

and 25 K is consistent with the rise of temperature activated susceptibility.¹ This corresponds presumably to the thermally activated population of triplet excitations. The separated lines A–C are distinctly seen in the temperature range 15–20 K: at lower temperatures, the intensity is weak because of the spin gap, and at higher temperatures, all signals merge into a single line.

The ESR absorption curves of the ceramic and aligned samples at close frequencies are given in Fig. 3. Dashed arrows near the curve of the ceramic sample mark the boundaries of the absorption band; A, B, and C denote the resonances appearing with heating. In contrast to ceramic samples, aligned samples show resonances at positions B and

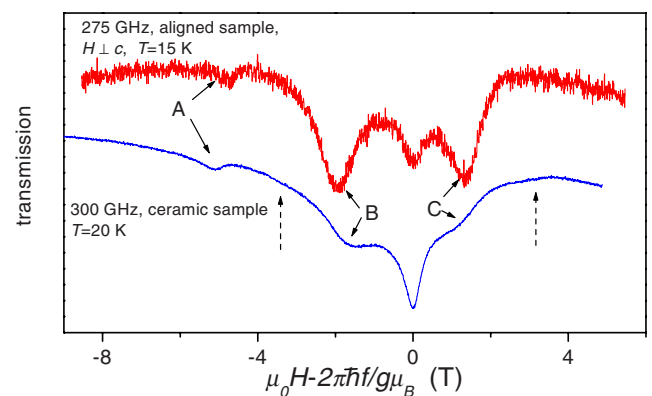


FIG. 3. (Color online) 300 GHz ESR spectrum of a $\text{PbNi}_2\text{V}_2\text{O}_8$ ceramic sample at $T=20$ K (lower curve) and 275 GHz spectrum of an aligned sample (upper curve).

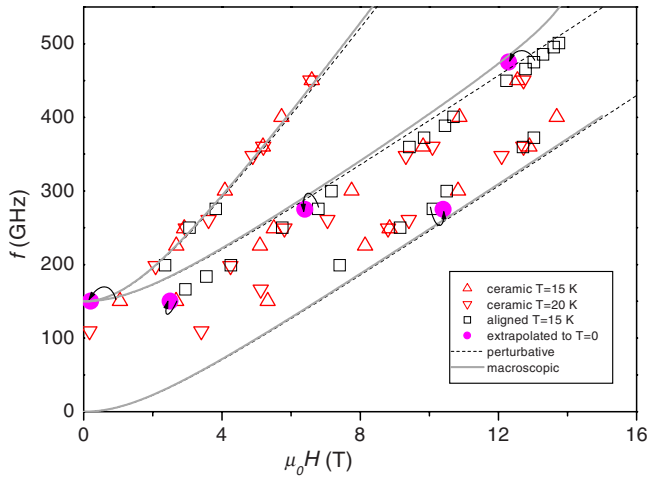


FIG. 4. (Color online) Frequency-field diagram of the thermally activated magnetic resonance of aligned samples at $\mathbf{H} \perp c$ and of ceramic samples. Triangles and squares present experimental data for resonances marked by A, B, and C. Lines are model calculations. Solid circles, noted by curved arrows, represent the extrapolations to $T=0$.

C, which exceed the defect peak placed between them. The resonance fields H_A , H_B , and H_C , taken at different frequencies, are plotted in Fig. 4. No absorption signal corresponding to the singlet-triplet transitions is observed.

The absorption, appearing with heating (lines A–C), corresponds approximately to the known ESR spectrum of $S=1$ ions in an axial crystal field (see, e.g., Ref. 7). For a uniaxial crystal, this ESR spectrum consists of three resonance lines corresponding to the transitions $|\pm 1\rangle \leftrightarrow |0\rangle$ with $\Delta S_z = \pm 1$ and $|-1\rangle \leftrightarrow |1\rangle$ with $\Delta S_z = \pm 2$. The resonance fields for a frequency f may be described in terms of a single-ion anisotropy constant D , which contributes to the Hamiltonian with the term $D\hat{S}_z^2$. At $2\pi\hbar f \gg D$, two of the resonance lines, corresponding to $\Delta S_z = \pm 1$, are on both sides of the free spin resonance field $\mu_0 H_0 = 2\pi\hbar f / g\mu_B$ and the distance between these two lines is $2D/g\mu_B$ for $\mathbf{H} \parallel c$ and approximately $D/g\mu_B$ for $\mathbf{H} \perp c$. The third line corresponds to a two-quantum transition, which is forbidden at $\mathbf{H} \parallel c$ and naturally has a smaller amplitude. For a powder (ceramic) sample, there should be a band of absorption instead of sharp resonance lines, the whole bandwidth is $2D/g\mu_B$, and the maxima of absorption are near the resonance field of crystallites with $c \perp \mathbf{H}$ because of their largest statistical weight (the field interval between maxima is again $D/g\mu_B$). The detailed analysis of powder sample ESR is given in Ref. 13. In the case of the easy plane anisotropy, the intensity of the lower field maximum is larger than that at the upper one because of a higher population of the lower spin sublevels. For the case of the easy-axis anisotropy, the relation between intensities should be inverted. The triplet character of the spectrum and the increase of the intensity with heating indicate that lines A–C are due to thermally activated triplet excitations of $\text{PbNi}_2\text{V}_2\text{O}_8$.

By applying the above consideration of a spin $S=1$ in a crystal field, we conclude that the effective anisotropy of the triplet excitations is of the easy plane type ($D_{\text{eff}} > 0$). Ac-

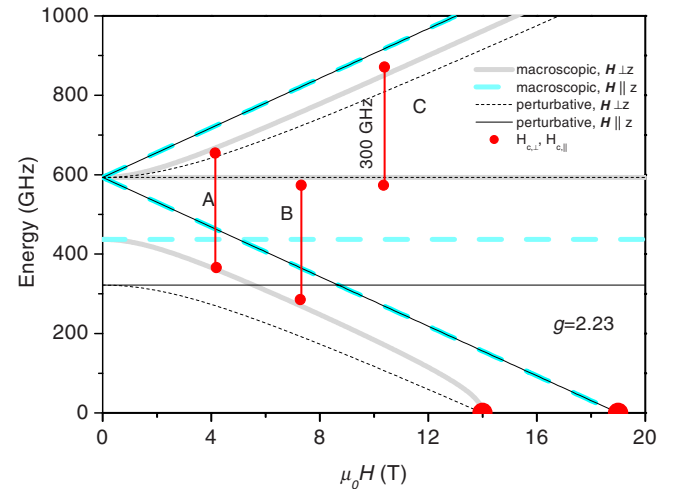


FIG. 5. (Color online) Triplet sublevels in a spin gap magnet with $\mu_0 H_{c\perp} = 14.0$ T and $\mu_0 H_{c\parallel} = 19.0$ T, calculated by the perturbative method (Ref. 4; thin lines) and in macroscopic models (Refs. 6 and 11; thick lines). Vertical segments present the observed transitions at $f=300$ GHz.

ording to Ref. 4, $D_{\text{eff}} \simeq -2D$; thus, the single-ion constant D should be negative, which agrees with the easy-axis anisotropy of the impurity induced ordered phase.¹² The maxima of the absorption are separated by approximately 3.5 T, which corresponds to $D_{\text{eff}} = g\mu_B\mu_0(H_C - H_B) \simeq 110$ GHz (hereafter, we assume $g=2.23$, as proved by ESR at $T > 35$ K). The leftmost absorption line demonstrates a characteristic frequency-field dependence (Fig. 4), with the asymptote $f = 2g\mu_B\mu_0 H / 2\pi\hbar$, marking a two-quantum transition with $\Delta S_z = \pm 2$. At $\mathbf{H} \perp c$, its zero-field limit should be equal to the zero-field splitting of the triplet components,⁷ i.e., D_{eff} . The observation of this absorption at the frequency of 150 GHz directly indicates that the splitting of the triplet sublevels by the effective crystal field is less than or about 150 GHz.

The perturbative approach yields by Eq. (1) the zero-field gaps $\Delta_{\parallel} = 320 \pm 10$ GHz and $\Delta_{\perp} = 590 \pm 10$ GHz. The corresponding splitting of 270 GHz is twice as large as estimated from the observed ESR lines. Alternatively, the energy levels of the triplet excitations can be calculated within the boson model.^{6,11} The details of calculations are given in Ref. 13. For $D_{\text{eff}} > 0$, the gaps are related to the critical fields as follows:

$$g\mu_B\mu_0 H_{c\perp} = \Delta_{\parallel}, \quad g\mu_B\mu_0 H_{c\parallel} = \Delta_{\perp}. \quad (2)$$

From the critical field values, we get here $\Delta_{\parallel} = 440 \pm 10$ GHz and $\Delta_{\perp} = 590 \pm 10$ GHz. The splitting of 150 GHz agrees much better with the experimental results. The calculated triplet sublevels for perturbative and boson macroscopic models are presented in Fig. 5. Here, the critical fields are locked to the observed values. The difference in Δ_{\parallel} values, calculated in two models, occurs mainly due to the very steep field dependence of the lowest sublevel near $H_{c\perp}$ given by macroscopic models. It should be noted that in low fields, i.e., far from the critical point, all models would dem-

onstrate identical results when they lock on the same energy gaps at $H=0$.

The frequency-field dependence for the case $H \perp c$ that is calculated in a perturbative approach and in the models of Refs. 6 and 11 is presented in Fig. 4. It should be noted that no fitting parameters are used here, the value of zero-field splitting, $D_{eff}=\Delta_{\perp}-\Delta_{\parallel}$, is taken from critical fields via relation (2). The resonance fields were taken at $T=15$ and 20 K, while critical fields are measured at 4.2 K. Thus, we have to extrapolate the observed resonance fields to zero temperature. The temperature evolution of the ESR spectra, which is analogous to that shown in Fig. 2, was followed for the frequencies 150 , 275 , and 475 GHz. The resonance fields, extrapolated to $T=0$, are shown in Fig. 4 by solid circles, pointed by arrows. The data, extrapolated to zero temperature, lie on the model curve within the experimental error. Note that the energy levels predicted in Refs. 1, 2, and 10, by using the model in Ref. 4 ($D_{eff}=270$ GHz and $\Delta_{\perp}=590$ GHz), do not correspond to the above experimental data to any extent.

The temperature dependence of the triplet ESR field observed in the present work may probably be attributed to the interaction between the triplets, analogous to the spin-wave frequencies in conventional ferro- and antiferromagnets, which are known to be renormalized with the excitation of magnons (see, e.g., Refs. 14 and 15). The temperature dependence of the triplet excitation spectrum was observed also for the dimer spin-gap compound $TiCuCl_3$.¹⁶ An alternative reason for the temperature dependence of D_{eff} and the triplet excitation spectrum may be the change of the correlation length with heating. However, according to experiments,¹⁷ the correlation length is reduced only by 20% at the tempera-

ture of half the intrinsic Haldane gap $0.41J$, as in our case. Apparently, this may not substantially change the effective anisotropy constant of triplet excitations. The excitation of the triplets apart from the bottom of the spectrum may not also change the position of the absorption maxima, despite having a smaller D_{eff} . As noted in Ref. 6, the influence of higher energy excitations will result in an asymmetric form of the ESR lines, but not in the shift of the absorption maximum.

In conclusion, the ESR spectrum of triplet excitations in a Haldane magnet $PbNi_2V_2O_8$ demonstrates a temperature dependence, probably due to the interaction between the excitations. The low-temperature ESR of triplet excitations is satisfactorily described without fitting parameters, using the experimental values of critical fields. The relation between the critical fields and energy gaps corresponds to the boson model of Ref. 6 and macroscopic theory,¹¹ and contradicts the fermion model of Ref. 6 and isolated chain calculations of Ref. 4. This supposedly indicates a strong influence of the 3D correlations on the spectrum of excitations in $PbNi_2V_2O_8$.

Authors are indebted to A. M. Farutin, V. I. Marchenko, T. Sakai, and M. E. Zhitomirsky for discussions. This work was, in part, supported by the Grant-in-Aid for Scientific Research on Priority Areas from the Japanese Ministry of Education, Culture, Sports, Science and Technology and by the Russian Foundation for Basic Research Grant No. 06-02-16509. Some of these studies were done under a Foreign Visiting Professor Program in KYOKUGEN, Osaka University.

-
- ¹Y. Uchiyama, Y. Sasago, I. Tsukada, K. Uchinokura, A. Zheludev, T. Hayashi, N. Miura, and P. Böni, *Phys. Rev. Lett.* **83**, 632 (1999).
- ²A. Zheludev, T. Masuda, I. Tsukada, Y. Uchiyama, K. Uchinokura, P. Böni, and S.-H. Lee, *Phys. Rev. B* **62**, 8921 (2000).
- ³T. Sakai and M. Takahashi, *Phys. Rev. B* **42**, 4537 (1990).
- ⁴O. Golinelli, Th. Jolicoeur, and R. Lacaze, *J. Phys.: Condens. Matter* **5**, 7847 (1993).
- ⁵L.-P. Regnault, I. A. Zaliznyak, and S. V. Meshkov, *J. Phys.: Condens. Matter* **5**, L677 (1993).
- ⁶I. Affleck, *Phys. Rev. B* **46**, 9002 (1992).
- ⁷A. Abragam and B. Bleaney, *Electron Paramagnetic Resonance of Transition Ions* (Clarendon, Oxford, 1970).
- ⁸M. Sieling, U. Löw, B. Wolf, S. Schmidt, S. Zvyagin, and B. Lüthi, *Phys. Rev. B* **61**, 88 (2000).
- ⁹N. Tsujii, O. Suzuki, H. Suzuki, H. Kitazawa, and G. Kido, *Phys. Rev. B* **72**, 104402 (2005).
- ¹⁰A. Zheludev, T. Masuda, K. Uchinokura, and S. E. Nagler, *Phys. Rev. B* **64**, 134415 (2001).
- ¹¹A. M. Farutin and V. I. Marchenko, *Zh. Eksp. Teor. Fiz.* **131**, 860 (2007) [*JETP* **104**, 751 (2007)].
- ¹²A. I. Smirnov, V. N. Glazkov, H.-A. Krug von Nidda, A. Loidl, L. N. Demianets, and A. Ya. Shapiro, *Phys. Rev. B* **65**, 174422 (2002).
- ¹³A. I. Smirnov, V. N. Glazkov, T. Kashiwagi, S. Kimura, M. Hagiwara, K. Kindo, A. Ya. Shapiro, and L. N. Demianets, arXiv:0708.1904 [cond-mat.str-el] (unpublished).
- ¹⁴F. Dyson, *Phys. Rev.* **102**, 1217 (1956); *Phys. Rev.* **102**, 1230 (1956).
- ¹⁵L. A. Prozorova and A. I. Smirnov, *Zh. Eksp. Teor. Fiz.* **74**, 1554 (1978) [*Sov. Phys. JETP* **47**, 812 (1978)].
- ¹⁶V. N. Glazkov, A. I. Smirnov, H. Tanaka, and A. Oosawa, *Phys. Rev. B* **69**, 184410 (2004).
- ¹⁷F. Tedoldi, R. Santachiara, and M. Horvatić, *Phys. Rev. Lett.* **83**, 412 (1999).